A low power miniaturized dielectric barrier discharge based atmospheric pressure plasma jet

G. Divya Deepak, N. K. Joshi, Dharmendra Kumar Pal, and Ram Prakash

Citation: Rev. Sci. Instrum. **88**, 013505 (2017); doi: 10.1063/1.4974101
View online: http://dx.doi.org/10.1063/1.4974101
View Table of Contents: http://aip.scitation.org/toc/rsi/88/1
Published by the American Institute of Physics

A low power miniaturized dielectric barrier discharge based atmospheric pressure plasma jet

G. Divya Deepak,[1] N. K. Joshi,[1] Dharmendra Kumar Pal,[2] and Ram Prakash[2]
[1]*Department of Nuclear Science and Technology, Mody University of Science and Technology, Lakshmangarh, Sikar 332311, India*
[2]*Plasma Devices Laboratory, CSIR-Central Electronics Engineering Research Institute, 333031 Pilani, India*

(Received 13 October 2016; accepted 2 January 2017; published online 18 January 2017)

In this paper, a dielectric barrier discharge plasma based atmospheric pressure plasma jet has been generated in a floating helix and floating end ring electrode configuration using argon and helium gases. This configuration is subjected to a range of supply frequencies (10-25 kHz) and supply voltages (2-6 kV) at a fixed rate of gas flow rate (i.e., 1 l/min). The electrical characterization of the plasma jet has been carried out using a high voltage probe and current transformer. The current-voltage characteristics have been analyzed, and the consumed power has been estimated at different applied combinations for optimum power consumption at maximum jet length. The obtained optimum power and jet length for argon and helium gases are 12 mW and 32 mm, and 7.7 mW and 42 mm, respectively. It is inferred that besides the electrode configurations, the discharge gas is also playing a significant role in the low power operation of the cold plasma jet at maximum jet length. The obtained results are interpreted on the basis of penning processes. *Published by AIP Publishing.* [http://dx.doi.org/10.1063/1.4974101]

I. INTRODUCTION

Dielectric barrier discharge (DBD) based atmospheric pressure plasmas have been used in numerous applications.[1–4] Atmospheric pressure plasma jets (APPJs) have received significant attention in recent time because they widen the plasma application range for biomedical purposes.[5,6] Different types of plasma jets have already been researched, relying on different excitation means from DC to microwave, and discharge mechanisms, such as capacitively coupled plasma discharge (CCP) and corona discharge,[7–10] but DBD based plasma jets have not been thoroughly explored.

Koinuma *et al.*[11] obtained a plasma jet at atmospheric pressure in a micro-beam plasma generator, which was later termed as "a 'cold' plasma torch" by Schütze *et al.*[12] In 2005, Laroussi and Lu[13] proposed a plasma jet with a cylindrical configuration fed by inert gases. They found that by confining the glow discharge in a tubular geometry with dimensions usually less than 1 cm in diameter, a stable discharge can be generated. Furthermore, APPJ is also investigated by Teschke *et al.*[14] by use of an intensified charge coupled device (ICCD) camera to capture photos of the jet with exposure time in 100 ns range. They have found that the presented plasma source acts like a "plasma gun" blowing small "plasma bullets" out of its mouth. Nie *et al.*[15] generated an argon plasma jet using a pair of tungsten pin electrodes, out of which only one was at floating potential. Nevertheless, a limited jet length is achieved despite working at higher operating voltage.

Jiang *et al.*[16] studied the effect of electrode configuration and discharge behavior on the helium plasma jet but have not conducted power consumption analysis of the device. Lei and Fang[17] analyzed the effect of gas flow on neon based APPJ generated using two planar electrodes which could be used for medical sterilization purposes. Xu *et al.*[18] fabricated a non-thermal plasma jet source, which produced helium plasma with an oxygen-rich atmosphere in a theta-shaped tube, and its potential was investigated for use in the topological alteration of plasmid DNA. This device consumed a peak power of 27 W at 7.5 kV/32 kHz discharge operation.

Recently portable plasma jet devices like jet needle and plasma pencil have also been constructed for their effective operation, and often molecular gases, such as oxygen or methane, are added to the inert carrying gases.[19–26] However, the electrical characterization of such discharges has not been carried out.

In this paper, an effort has been made by developing an APPJ using a new electrode arrangement consisting of the floating helix and end ring electrode. These two floating electrodes have been used to propagate the plasma jet to greater lengths at lower operating power. Peak power consumed by the developed APPJ is only of the order of few mW. The electrode configuration implemented shows low voltage operation and also high stability. The electrical characterization has been carried out for argon and helium gases. The developed APPJ has been studied with respect to the peak discharge current, jet length, and power consumed. The optimum power for maximum jet length is achieved for the helium gas in the proposed novel geometry.

II. GEOMETRY AND EXPERIMENTAL SETUP

The developed APPJ in a floating helix and floating end ring electrode configuration is shown in Fig. 1. The main body of the jet consists of a quartz tube of diameter 4 mm, which is used as a dielectric barrier between the electrodes. In this geometry, a pin electrode of diameter 1 mm and length 88 mm is used as a cathode, which is hermetically sealed with the quartz tube. The effective length of the pin electrode inside the quartz tube is 40 mm. The quartz tube is glass blown

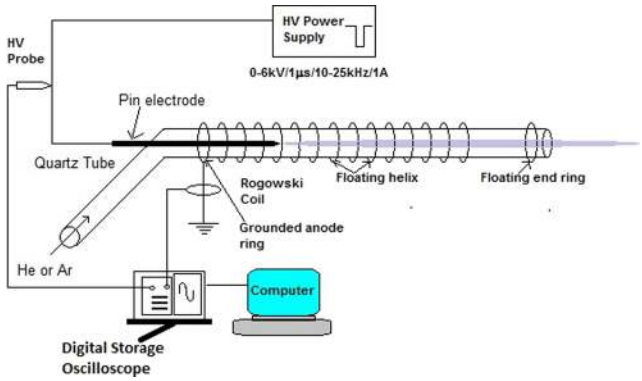

FIG. 1. Experimental setup of the floating helix electrode configuration but with the floating end ring.

in L-shape, so as to make an effective length of 123 mm for plasma discharge. The one end of the tube having length 30 mm is used for the gas connection whereas the other open end is used for a cold plasma jet outlet. A conductive epoxy silver foil tape of width 2 mm and 0.1 mm thickness tightly bound to the quartz tube at the gas inlet end is used as an anode, which is grounded. A fourteen turn helix of the same silver foil tape having pitch 5 mm has also been used as a plasma jet guiding rail. The pitch of the helix electrode in the guiding rail has been optimized experimentally based on the diffused discharge to occur between the successive helix pitches, and the number of turns has been decided to facilitate the propagation of the plasma jet out of the quartz tube.

The floating helix electrode causes charge accumulation on the dielectric surface around the helix and provides a subsequent discharge path for the plasma jet. Nevertheless, this floating helix electrode geometry electrode has provided a distortion in the plasma jet. So, to focus the plasma jet, another electrode of the same conductive epoxy silver foil tape has been used at the end of the quartz tube outlet after a gap of 25 mm from the helix. To understand the role of the floating end ring electrode on the plasma jet extraction for the same applied conditions, the end ring electrode has been removed in another case. The schematic view of the experiment without the end ring electrode is shown in Fig. 2. The experiments have been performed using two different gases, such as argon and helium, blown with 1 l/min gas flow

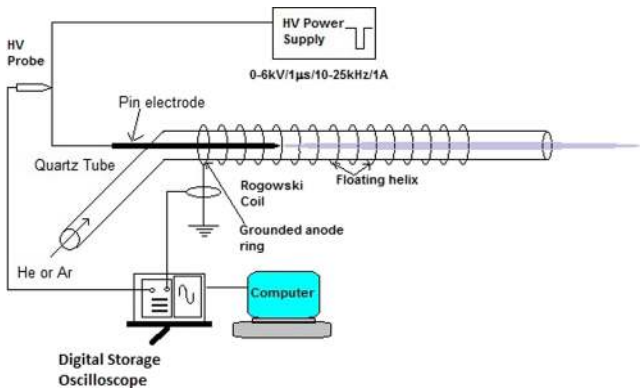

FIG. 2. Experimental setup of the floating helix electrode configuration but without the floating end ring.

FIG. 3. Argon jet generated using the floating helix configuration.

rate for all the experiments in an airtight arrangement in the atmospheric pressure environment. The gas discharge in this geometry has been studied for a range of supply frequency 10-25 kHz and supply voltage 2-6 kV operation. Accordingly the effect of jet length enhancement at optimum operating parameters has been analyzed for the aforementioned two APPJ configurations.

The applied voltage and currents are measured by using a high voltage probe (Tektronix P 6015 A; bandwidth 0-75 MHz) and Rogowski-type Pearson current monitor (Model 110; 0.1VA–1, 1 Hz–20 MHz, 20 ns usable rise time) connected to a digital storage oscilloscope (Tektronix DPO 4054; bandwidth 500 MHz). The plasma jets generated using the floating helix configuration along with the floating end ring for argon and helium gases are shown in Figs. 3 and 4, respectively.

In the discharge experiments, a plasma jet length up to 42 mm has been achieved from the open end of the quartz tube for the helium gas. The maximum effective length obtained in this configuration from the cathode tip is 122 mm.

III. RESULTS AND DISCUSSION

A. Experimental results of argon APPJ with floating helix electrode

A typical current-voltage (I-V) characteristic of the developed APPJ with a floating helix electrode for the argon gas is shown in Fig. 5. This figure also shows the calculated

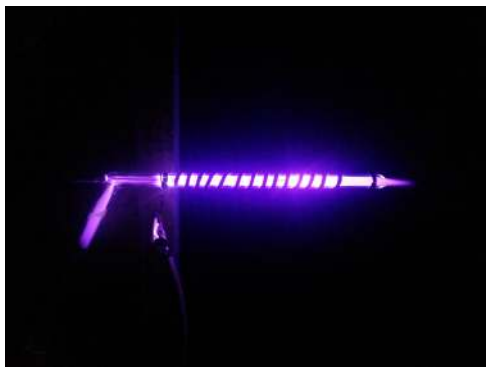

FIG. 4. Helium jet generated using the floating helix configuration.

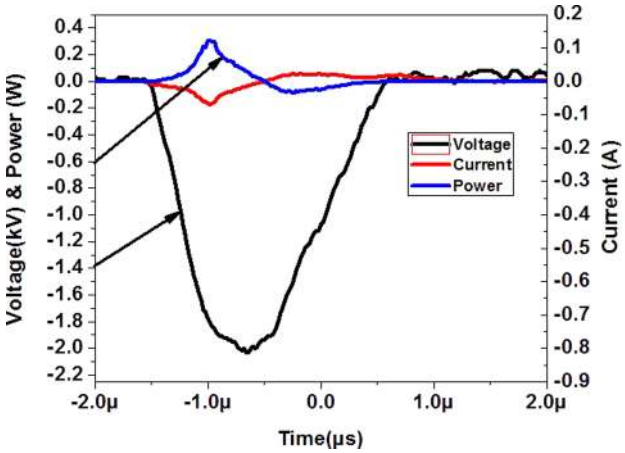

FIG. 5. Current-voltage (I-V) characteristic of the developed APPJ with the floating helix electrode at 2 kV/20 kHz (argon gas).

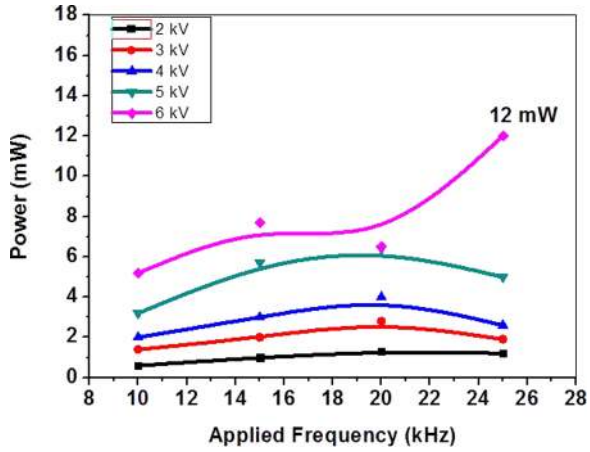

FIG. 6. Variation of power consumed at different frequencies and at different applied voltages with the floating helix electrode.

power from the I-V characteristics. We have used a unipolar square wave form voltage of 1 μs duration, where we do not have a smooth flat top region. It is well-known that in the dielectric barrier discharges with unipolar pulse operation only rising and falling flank are used in the DBD discharge,[27] and hence we could not stress much on the smooth flat top region. Furthermore, we have worked in a self-breakdown condition of discharge; therefore, the measured I-V characteristics presented here have not been averaged over a large number of pulses rather than the taken snapshot of a single pulse. The definite time integral of the power for the applied pulse duration has produced energy consumed per pulse (in joules). In this case, the estimated value of energy consumed per pulse at jet operational parameters 2 kV/20 kHz is 6.5×10^{-8} J. Accordingly the power consumed by the device has been estimated by multiplying the energy consumed per pulse with the applied frequency, which yields 1.3 mW consumed power in the argon APPJ with the floating helix electrode. An explanation for the phenomenon of current reversal that is seen in the I-V characteristic could be found elsewhere.[27]

The variation of the consumed power for different applied frequencies and voltages is shown in Fig. 6, which varies from 0.6 mW to 1.3 mW for a range of frequencies from 10 at 25 kHz for the same applied voltage 2 kV. A uniform discharge occurs all along the surface of the cathode and due to increment in the frequency, the inherent collision process increases, which leads to a better discharge condition. It is observed that at supply voltages 2-5 kV, there is a linear relationship between the power consumed and supply frequency till 20 kHz. But when the supply frequency is increased further to 25 kHz, there is a decrement in the power consumed. This is due to memory charges that can cause further ionization of argon gas atoms[27] and thus resulting in reduced power.

At higher voltage, i.e., 6 kV for the supply frequency range 10-15 kHz, the power consumed has increased again because the input energy is lost as heat in the dielectrics. Interestingly when the supply frequency is increased further to a range of 20-25 kHz at 6 kV applied voltage, the power consumed by the APPJ has shown sudden increase in the power consumption from 6.5 mW to 12 mW. This sudden rise of power consumed is perhaps due to multiple steamer formation.[28] Eventually at higher voltages and frequencies (6 kV/25 kHz), there occurs multiple peak discharge phenomenon, which is also clearly visible in the current waveform with multiple peaks as shown in Fig. 7.

When a floating end ring is introduced to argon APPJ with the floating helix electrode, it resulted in a more uniform discharge, which can be seen from the single peak discharge occurrence in the current waveform even at 6 kV/20 kHz (see Fig. 8).

Figs. 9 and 10 depict the jet lengths as a function of supply frequencies for different applied voltages estimated for the cases of without and with the floating end ring electrodes. There is a linear relationship between jet lengths and supply frequencies at all applied voltages. Nevertheless, the rate of jet length enhancement is maximum when the supply frequency is increased from 20 to 25 kHz at higher voltages. This is again due to the sudden increase in the consumed power of the APPJ at these frequencies at higher voltages. The maximum jet length of 32 mm has been observed at 6 kV/25 kHz with the floating end ring electrode whereas without the floating

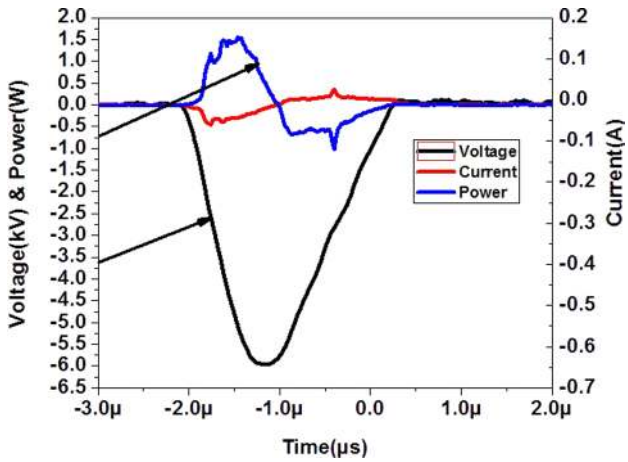

FIG. 7. Current-voltage (I-V) characteristic of the developed APPJ with the floating helix electrode at 6 kV/25 kHz (argon gas).

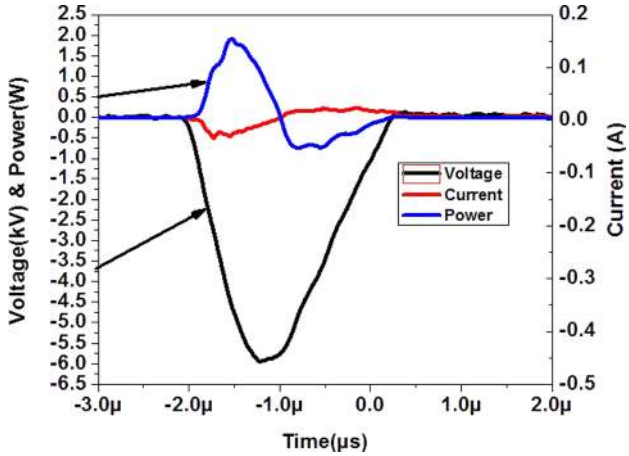

FIG. 8. Current-voltage (I-V) characteristic of the developed APPJ with the floating helix electrode and floating end ring configuration at 6 kV/20 kHz (argon gas).

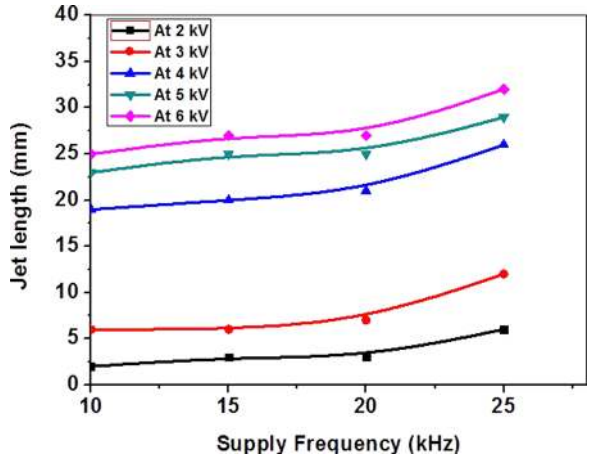

FIG. 10. Variation of plasma Jet length at different supply frequencies and different voltages for the argon gas (with end ring).

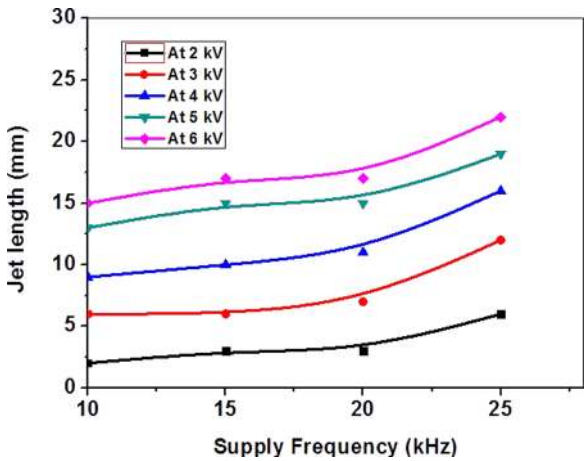

FIG. 9. Variation of plasma Jet length at different supply frequencies and different voltages for the argon gas (without end ring).

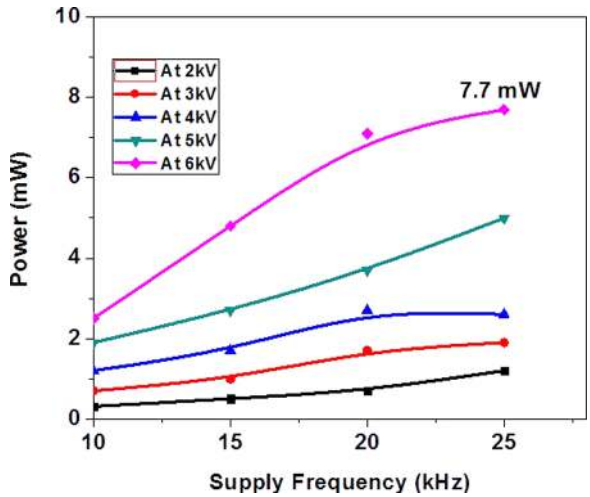

FIG. 11. Variation of power consumed at different supply voltages and different supply frequencies for the floating helix electrode (helium gas).

end ring electrode, the jet length is 22 mm at the same applied conditions. This difference in the jet length is due to charge accumulation that happens along the surface of the dielectric due to the presence of end ring floating sheath.[29] In fact, the floating sheath has provided an additional support and accordingly has enhanced the plasma jet length as seen in Fig. 10. At low supply frequency up to 10 kHz and lower voltage up to 3 kV, there is no significant effect of the floating end ring electrode on the jet length (see Figs. 9 and 10). But, when the voltage is increased beyond this limit, the length of the plasma jet has increased substantially for the floating end ring electrode condition (see Fig. 10). The length of the plasma has increased by the floating plasma sheath and its associated electric field at the quartz tube outlet, which resulted in a clearly seen increased jet length of 6 mm compared to one without the floating end ring electrode.

B. Experimental results of helium APPJ using floating helix electrode

Fig. 11 shows the variation of power consumed by the plasma discharge as a function of supply frequency at different voltages for the helium gas using the floating helix electrode. It is seen that at lower applied voltages 2-4 kV there is no much difference in the power consumed because uniform discharge occurs all along the cathode surface. However, at higher applied voltages, i.e., 5-6 kV, the rate of power consumed has rapidly increased for the supply frequency range 20–25 kHz, which is yet again due to substantial power losses in the dielectrics. The peak power consumed at 6 kV/25 kHz is 7.7 mW for the helium gas and has been estimated using I-V characteristics from Fig. 12, which shows ~35% reduction in the consumed power for the change of gas from argon to helium for the same applied conditions.

For the floating helix and floating end ring configuration, the power consumed is ~8 mW and is shown in Fig. 13. We were limited by the power supply, but still it can be argued that there is a critical limit of supply voltage and frequency after which the input energy is not used for sustaining the plasma discharge. The input energy is lost in the thermal dissipation to the dielectric material and also heating of helium gas atoms which is indicated by the sudden rise in the power consumed for higher voltages (5-6 kV) and supply frequencies (20-25 kHz).

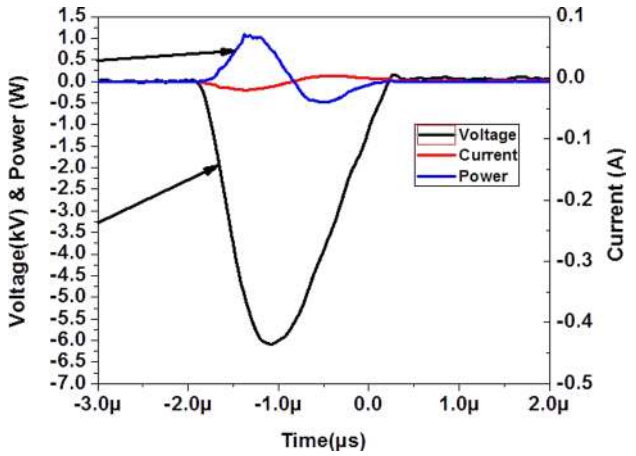

FIG. 12. Current-voltage (I-V) characteristic of the developed APPJ with the floating helix electrode at 6 kV/25 kHz (helium gas).

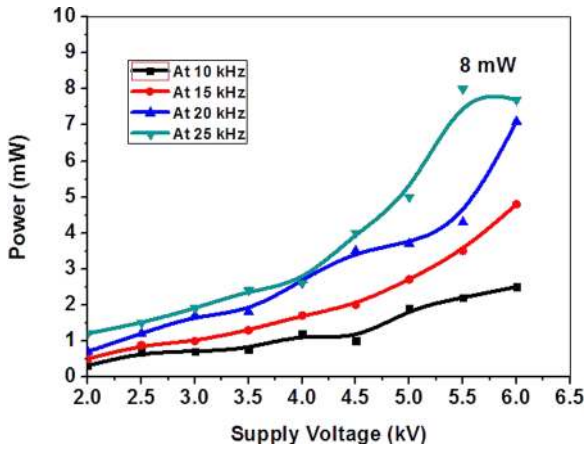

FIG. 13. Variation of power consumed at different supply voltages and different supply frequencies for floating helix and floating end ring electrodes (helium gas).

The jet lengths achieved at different supply voltages without and with the floating end ring electrode are compared for the helium gas and are shown in Figs. 14 and 15, respectively. It is clearly seen that the plasma jet length is more for the case of with the floating end ring electrode as compared to that one without the end ring electrode. The floating electrode helps in charge accumulation resulting in jet length enhancement for the same input conditions of the supply voltage and frequency. The effect of the floating end ring electrode near the quartz tube outlet at a lower frequency of 10 kHz is not seen till a voltage of 2.5 kV but when the voltage is increased further to 3 kV, there is an enhancement in the jet length of about 2 mm as compared to the one without the floating end ring configuration. This effect of an increase in plasma jet length is due to the fact there is an electric force that is created by the end ring at the floating electrode by means of charge accumulation and the gas flow of the APPJ pulls plasma jet towards the quartz tube outlet.

The effect of jet length enhancement is more at higher supply voltages. This is because electrons gain more energy resulting in more ionization and also expansion of luminous spots on the cathode occurs.[31] For higher voltage and frequency (i.e., 6 kV/25 kHz), the effect of jet length

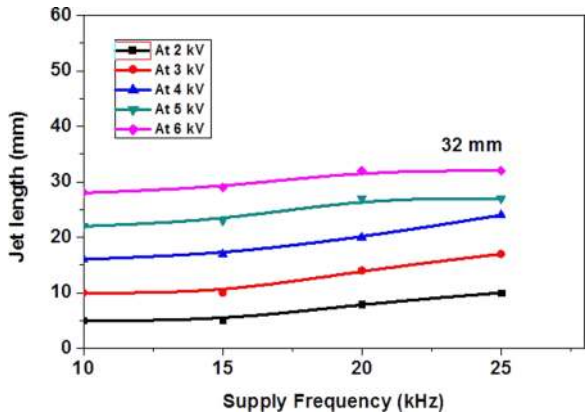

FIG. 14. Jet length vs supply frequency at different voltages (without end ring) for the helium gas.

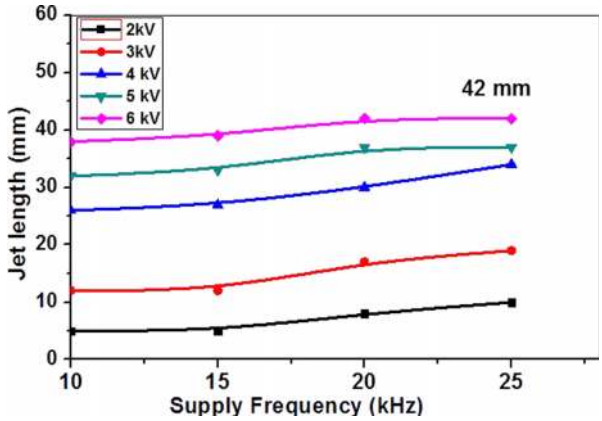

FIG. 15. Jet length vs supply frequency at different voltages (with end ring) for the helium gas.

enhancement is 10 mm because more energetic electrons are available due to high field to cause ionisation of the gas atoms and thus resulting in greater lengths of plasma jets (see Fig. 15).

Eventually the length of the helium plasma jet is more than that of the argon plasma jet as the ionization potential of He is 24.6 eV as compared to 15.6 eV for the argon gas. Therefore, it is easier for the helium to get ionized to generate ions at the He/Air interface via penning process.[30] Actually the high energy metastable states of helium cause more penning ionization of atoms to form ions than that of the argon gas near the air interface. The electrons freed in this process acts as seed electrons for the succeeding electric avalanches. The Ar atoms have lower energy and their capability of causing penning ionization is smaller. The discharge proceeds via the streamer process to generate filamentous plasma between the electrodes and discharge current is quite high as the resistance of the discharge channel is low. Our experimental results are in confirmation with the cold plasma jet results obtained by Shao *et al.*[31] proving that the argon plasma jet consumes more power compared to the helium plasma jet.

IV. SUMMARY

Atmospheric pressure plasma jet has been generated in a floating helix and end ring electrode arrangement using argon

and helium gases separately. The peak power consumed by the configuration where both the floating helix and end ring configurations are used is 12 mW at 6 kV/25 kHz for the argon gas. Even though the jet length is a function of supply voltage and frequency, our experiments show that the jet length is also affected by the presence of the floating end ring electrode. The maximum jet lengths of 32 mm (with floating end ring electrode) and 22 mm (without floating end ring electrode) have been achieved at 6 kV, 25 kHz for the argon gas.

From the experimental results of the helium plasma jet, the power consumed is found to be 8 mW at 5.5 kV, 25 kHz. Furthermore, the maximum jet lengths of 42 mm (with floating end ring electrode) and 32 mm (without floating end ring electrode) have been achieved at 6 kV, 25 kHz for the helium gas case. It is found that the floating end ring electrode is beneficial to control the discharge, especially it restricts the transition of glow discharge to arc discharge in a cold plasma jet configuration. It further helps in lowering the power consumption and greater jet length creation. It is evident that the length of the helium plasma jet is more than that of the argon plasma jet, which has been explained on the basis of Penning process. The practical applications of the developed floating electrode DBD with longer jet lengths and lower power operations can be realized for the direct plasma treatment on skin and also for the surface treatment of traditional art and craft. However, this will require *in vitro* biomedical laboratory testing and study of biomedical changes and other sterilizing effects to establish the relevance.

ACKNOWLEDGMENTS

The author, G. Divya Deepak, thanks Dean C.E.T. (Mody University of Science and Technology) for his encouragement and support during this work. He also thankfully acknowledges the Director, CSIR-Central Electronics Engineering Research Institute, Pilani for providing necessary lab facilities in performing these experiments.

[1]B. Eliasson and U. Kogelschatz, IEEE Trans. Plasma Sci **19**, 309 (1991).
[2]V. I. Gibalov and G. J. Pietsch, J. Phys. D: Appl. Phys. **33**, 2618 (2000).
[3]U. N. Pal, P. Gulati, N. Kumar, R. Prakash, and V. Srivastava, IEEE Trans. Plasma Sci. **40**, 1356 (2012).
[4]I. Radu, R. Bartnikas, G. Czeremuszkin, and M. Wertheimer, IEEE Trans. Plasma Sci. **31**, 411 (2003).
[5]J. Rahel and D. M. Sherman, J. Phys. D: Appl. Phys. **38**, 547 (2005).
[6]M. Thomachot and L. Marlin, Plasma Source Sci. Technol. **15**, 828 (2006).
[7]U. N. Pal, P. Gulati, N. Kumar, M. Kumar, M. S. Tyagi, B. L. Meena, A. K. Sharma, and R. Prakash, IEEE Trans. Plasma Sci. **39**, 1475 (2011).
[8]R. Valdivia-Barrientos, V. Pacheco-Sotelo, M. Pacheco-Pacheco, J. S. Benítez-Read, and R. López-Callejas, Plasma Sources Sci. Technol. **15**, 237 (2006).
[9]G. Divya Deepak, N. K. Joshi, U. Pal, and R. Prakash, Laser Particle Beams **34**, 615 (2016).
[10]A. Flores-Fuentes, R. Peña-Eguiluz, R. López-Callejas, A. Mercado-Cabrera, R. Valencia-Alvarado, S. Barocio-Delgado, and A. de la Piedad-Beneitez, IEEE Trans. Plasma Sci. **37**, 128 (2009).
[11]H. Koinuma, H. Ohkubo, T. Hashimoto, K. Inomata, T. Shiraishi, A. Miyanaga, and S. Hayashi, Appl. Phys. Lett. **60**, 816 (1992).
[12]A. Schütze, J. Y. Jeong, S. E. Babayan, J. Y. Park, G. S. Selwyn, and R. F. Hicks, IEEE Trans. Plasma Sci. **26**, 1685 (1998).
[13]M. Laroussi and X. Lu, Appl. Phys. Lett. **87**, 113902 (2005).
[14]M. Teschke, J. Kedzierski, E. G. Finantu-Dinu, D. Korzec, and J. Engemann, IEEE Trans. Plasma Sci. **33**, 10 (2005).
[15]Q.-Y. Nie, C.-S. Ren, D.-Z. Wang, and J.-L. Zhang, Appl. Phys. Lett. **93**, 011503 (2008).
[16]N. Jiang, A. Ji, and Z. Caoa, J. Phys. D: Appl. Phys. **106**, 013308 (2009).
[17]X. Lei and Z. Fang, IEEE Trans. Plasma Sci. **39**, 2288 (2011).
[18]G.-M. Xu, Y. Ma, and G.-J. Zhang, IEEE Trans. Plasma Sci. **36**, 1352 (2008).
[19]J. Y. Kim, D.-H. Lee, J. Ballato, W. Cao, and S.-O. Kim, Appl. Phys. Lett. **101**, 22410 (2012).
[20]M. Laroussi and T. Akan, Plasma Processes Polym. **4**, 777 (2007).
[21]D. Dudek, N. Bibinov, J. Engemann, and P. Awakowicz, J. Phys. D: Appl. Phys. **40**, 7367 (2007).
[22]X. P. Lu, Z. H. Jiang, Q. Xiong, Z. Y. Tang, and Y. Pan, Appl. Phys. Lett. **92**, 151504 (2008).
[23]J. Shi, F. Zhong, J. Zhang, D. W. Liu, and M. G. Kong, Phys. Plasmas **15**, 013504 (2008).
[24]B. L. Sands, B. N. Ganguly, and K. Tachibana, IEEE Trans. Plasma Sci. **36**, 956 (2008).
[25]B. L. Sands, B. N. Ganguly, and K. Tachibana, Appl. Phys. Lett. **92**, 151503 (2008).
[26]F. Massines and G. Gouda, J. Phys. D: Appl. Phys. **31**, 3411 (1998).
[27]U. N. Pal, P. Gulati, R. Prakash, V. Srivastava, and S. Konar, Plasma Sci. Technol. **15**, 635 (2013).
[28]Z. Chen, G. Xia, Q. Zhou, Y. Hu, X. Zheng, Z. Zheng, L. Hong, P. Li, Y. Huang, and M. Liu, Rev. Sci. Instrum. **83**, 084701 (2012).
[29]K.-U. Riemann, J. Phys. D: Appl. Phys. **24**, 493 (1991).
[30]Y. P. Raizer, *Gas Discharge Physics* (Springer-Verlag, Germany, 1991), p. 178.
[31]X.-J. Shao, N. Jiang, G.-J. Zhang, and Z.-x. Cao, Appl. Phys. Lett. **101**, 253509 (2012).